

Review

Thin-film coating methods: A successful marriage of high-quality and cost-effectiveness- A brief exploration

Muhammad A. Butt

¹ Warsaw University of Technology, Institute of Microelectronics and Optoelectronics, Koszykowa 75, 00-662 Warszawa, Poland
Correspondence: ali.buttpw.edu.pl (M.A.B)

Abstract: In this review, several cost-effective thin-film coating methods which include dip-coating, spin-coating, spray-coating, blade-coating, and roll-coating are presented. Each method has its set of advantages and disadvantages depending on the type of application. Not all of them are appropriate for large-scale production due to their certain limitations. That is why the coating method should be selected based on the type and size of substrate including the resolution of the required thin-films. The sol-gel method offers several benefits, such as simplicity in fabrication, excellent film uniformity, the capacity to cover surfaces of any size and over vast areas, and a low processing temperature. Nevertheless, these coating methods are somewhat economical and well managed in low-budget laboratories. Moreover, the produced thin-films are homogeneous and have low-surface roughness. Furthermore, some other thin-film deposition methods such as physical vapor deposition (PVD) and chemical vapor deposition (CVD) are also discussed. Since CVD is not restricted to line-of-sight deposition, a characteristic shared by sputtering, evaporation, and other PVD processes, many manufacturing methods favor it. However, these techniques require sophisticated equipment and cleanroom facility. We aim to provide the pros and cons of thin-film coating methods and let the readers decide the suitable technique for their specific application.

Keywords: Dip-coating; spin-coating; roll-coating; blade-coating; spray-coating; physical vapor deposition; chemical vapor deposition; flame hydrolysis deposition; sputtering.

1. Introduction

The coating is the way of incorporating a thin coating of material to a substrate by deposition in either the liquid phase (solution) or the solid phase (powder or nanoparticles) [1]. The use of coating strategies may be tailored to meet production requirements for coated layer thickness, coated surface roughness, rate, and coating product size, which can be defined by coating velocity, coated film width, and patterning capabilities [2]. The coating operation may be carried out at air pressure and low vacuum conditions. It is categorized according to the solubility of the coating components used. In solution coating, a binder and target material are dissolved in a solution that may coat the substrate directly, and the solution then evaporates from the resultant wet film to produce a dry film. As opposed to this, vacuum deposition techniques including chemical vapor deposition (CVD) [3], physical vapor deposition (PVD) [4], atomic layer deposition (ALD) [5], plasma [6], flame hydrolysis deposition (FHD) [7, 8], and sputtering [9] are mostly used to produce thin, uniform metallic layers that are utilized to transfer heat or electricity under low- or high-vacuum conditions. The guiding layer must have a higher refractive index than the substrate and cladding to effectively confine light [10, 11]. Consequently, thin-film deposition and local bulk material manipulation are the two major methods that may be used to execute the guiding layer. The thin-layer deposition method includes procedures such as RF-sputtering and magnetron sputtering, CVD, plasma-enhanced CVD, FHD, spray pyrolysis deposition, pulsed laser deposition, spin-coating, spray-coating, and sol-gel coating. The direct inscription of a channel WG in the substrate using an fs-

laser is an alternative to performing local modifications of the bulk material via ion exchange, ion implantation, or UV radiation.

Using the roll-coating process, a surface is coated with a tiny, micro nanoscale layer of liquid that has been recirculated across a sheet or web. The major goal of the thin layer coating is to increase the surface's effectiveness, service life, and quality. The coating is widely employed at the industrial level due to its useful benefits and applicability. The manufacturing of paper, paperboard, cellulose thin films, plastic coatings, fibrous fabric sheets, metallic foils, etc. are only a few of the processes in which it is primarily utilized. Most of the chemicals employed in the roll-coating procedure are non-Newtonian fluids that behave in either a viscoelastic or pseudoelastic manner [12, 13].

Due to its effective material utilization and direct and accurate patterning with a resolution of 20-30 mm, in contrast to spin-coating as well as other traditional processes, ink-jet printing techniques have drawn interest as a potentially cost-effective way for fabricating Perovskite solar cells (PSCs) [14, 15]. Regrettably, because of its complexity and poor volume output, ink-jet printing cannot be easily adapted to mass production [16]. With no restrictions on substrate size and minimal polymer use, spray-coating techniques offer a promising future for large-scale manufacturing [17]. They are expected to replace spin-coating methods, the industry standard. The ability to access a wide range of fluids with different rheology makes it possible to produce completely spray-coated PSC devices. However, the use of spray coating in the manufacture of PSC is constrained by a major problem: a thicker and more uneven layer [18]. Therefore, most current research focuses on improving the morphology of an active layer employing high boiling point solvents [19], additives, solvent combinations, post thermal annealing, and other spray coating techniques [19].

Spin-coating is a rapid and popular method for depositing thin films on substrates, and its main benefit is that it is simple to create extremely uniform films. When a solution of a particular substance is spun at a fast speed, the centripetal force and the liquid's surface tension work together to cover the substrate uniformly. Spin-coating produces a thin film with a thickness of a few nanometers to a few microns after the surplus solvent is removed. Small substrates that range in size from a few millimeters square to a meter or more in diameter are coated using the spin-coating process. The convenience and relative ease of setting up the process, together with the thinness and homogeneity, are the main benefits of the spin-coating approach.

The dip-coating technique is a quick, easy, affordable, and high-quality coating method utilized in both industrial and lab applications [20]. The dip-coating method is frequently used for optical coatings, including large-area antireflective coating for sun control glasses and the manufacture of vehicle rear mirrors. In the dip-coating procedure, a substrate is submerged in a solution of coating components before the solution is drained away. The procedure may be described as the solution-based deposition of an aqueous-based liquid phase onto a substrate's surface. The requisite material is typically dissolved in solutions and directly applied to the substrate surface. There are several complicated chemical and physical variables used in the dip-coating process. The duration of immersion, speed of withdrawal, dip-coating cycles, density and viscosity, surface tension, substrate surface, and coating solution evaporation factors all affect the thickness and shape of the film.

The paper is arranged subsequently: **Section 2** presents the basic mechanism and the recent advancements in the dip-coating method. It is one of the easiest and most common methods for producing thin films from a wide range of inorganic, hybrid, and nanocomposite materials. In the spin-coating method, a tiny drop of coating material is put into the substrate's center before the substrate is rotated at a regulated high speed. The size of the substrate is one of the key drawbacks of spin-coating. High-speed spinning is more challenging as the size goes up since film thinning gets more challenging. The working mechanism and recent progress in this technology are presented in **Section 3**. Roll-coating is a pre-metered coating that applies coating liquid to a substrate using a succession of rollers. The amount of coating material provided to the substrate is practically independent of the

characteristics and structures of the fabric because a metered layer of the coating liquid is first generated on the roller surface before it is transferred to the substrate as discussed in **Section 4**. **Section 5** presents the traditional spray-coating method that is still the most often reported due to its low cost and lack of specialized equipment, though. Some equipment is connected to compressors for photocatalytic coating so that the solution exists at the desired speed and pressure. Like the dip-coating technique, the solution must be correctly prepared before being loaded into the spray. Blade coating offers the benefit of large-area homogeneity, little material waste, interlayer dissolution prevention, compatibility with roll-to-roll manufacturing, and more efficient use of active material while still allowing for the preparation of well-defined films as discussed in **Section 6**. Moreover, there are several other noteworthy physical and chemical deposition methods available and being widely used in research and industry such as physical vapor deposition (PVD) and chemical vapor deposition (CVD) are also discussed in **Section 7**. And the paper ends with a fine discussion and the author's opinion on coating methods in **Section 8**. For quick navigation of the paper content, the graphical illustration is given in **Figure 1**.

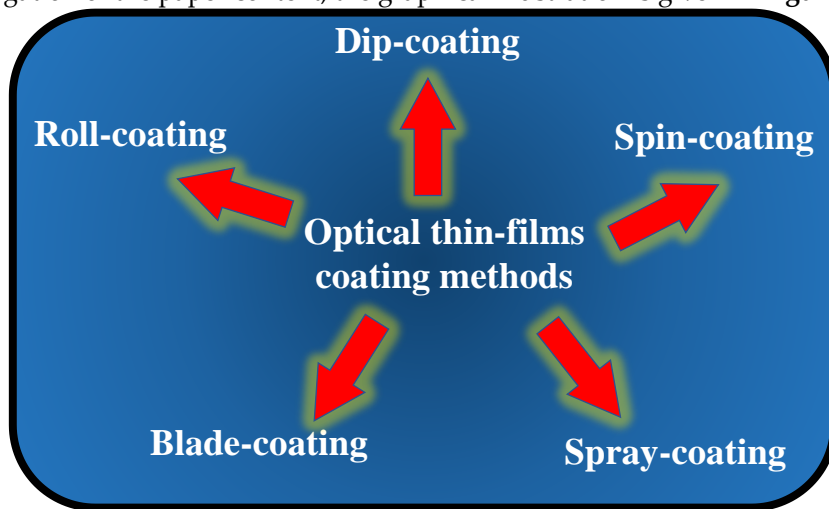


Figure 1. Graphical illustration of the optical thin-films coating methods discussed in this review.

2. Dip-coating

One of the easiest and most common methods for producing thin films from a wide range of inorganic, hybrid, and nanocomposite materials is the sol-gel method [21, 22, 23]. Considering that it provides for coating a broad range of substrates and complicated geometries, including substrates with holes or intricate patterns, it provides for a high degree of control over the crucial parameters and offers flexibility that cannot be achieved with other traditional processes. There are several ways for wet thin-film coating, namely dip-coating [24, 25], spin-coating [26], spray coating [27], and flow coating [28], among others. Fundamentally, the substrate to be coated is submerged in the initial solution and then pulled out at a consistent withdrawal speed during the process, which is carried out under well-controlled temperature and air conditions. A fine-tuning of the film properties, including thickness, optical constants, and interior structure, is made feasible by precisely controlling the withdrawal speed and the evaporation circumstances. The solution uniformly spreads out along the surface of the substrate because of the combined effects of viscous drag and capillarity action. Evaporation takes place at the process' last stage, resulting in the gelation of the film. The coated substrates often get a post-heat treatment, which affects the properties of the films [29]. The dip-coating process is shown in **Figure 2**.

The effectiveness of the dip-coating process can be directly impacted by several factors, such as pH and solution concentration, by changing, for example, its viscosity. However, as contemporary studies employ coating procedures that have already been documented in earlier works, most authors don't talk much about pH and solution viscosity.

Fewer repetitions of the dip-coating process are required to produce a certain thickness or amount of deposited mass when using more viscous solutions since they lead to greater agglomeration and thicker layers of coating [30]. However, the resultant coating could potentially break and clump particles in undesirable places. To get past these issues, the dip-coating technique can provide a more homogenous coating by using a less viscous solution in combination with multiple repeats. The structure's rate of immersion in the solution is yet another factor that might affect the coating's features [31]; a high rate of immersion, for example, may produce thicker layers because the solution's viscous forces are increased, causing greater accumulation on the structure's surface [32].

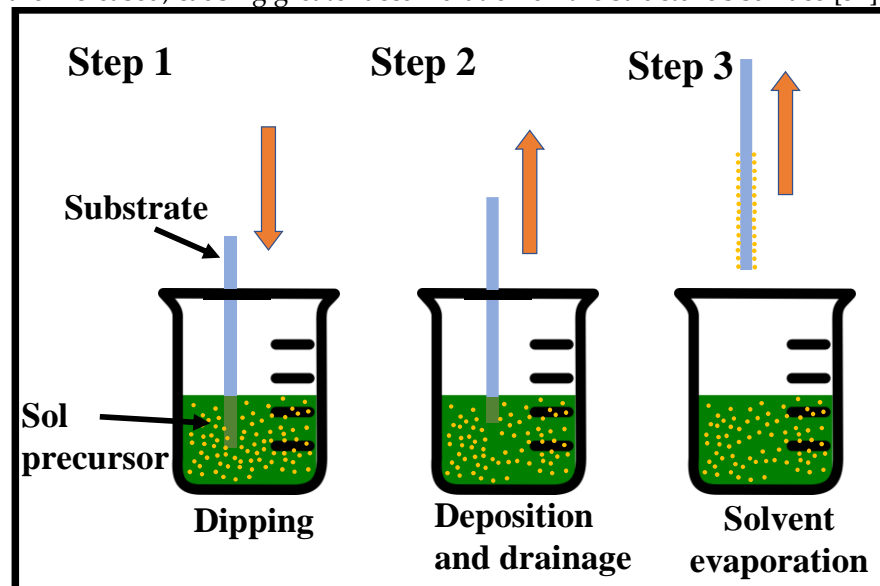


Figure 2. Sequential stages of the sol-gel dip-coating method for thin film deposition: Stage 1- the substrate is dipped and immersed in the sol precursor, Stage 2- the substrate is withdrawn at a steady rate, Stage 3- Solvent evaporation produces the gelation of the layer.

For thin-film coating techniques to be employed successfully in integrated optics, the film thickness must be completely under control. Because of this, thickness control is important for all thin-film development methods, including sol-gel. It has been reported that the coating speed, angle of inclination, and sol concentration have a major role in determining the ultimate thickness [33, 34, 35]. In addition, the ultimate heat-treated thickness can also be influenced by the sol viscosity, density, and liquid-vapor surface tension [36]. In [37] it is stated that a cleanroom atmosphere is required for the coating procedure to produce sol-gel thin films with great optical quality. To produce organic dye-doped thin films with tailored porosity for use in chemical sensing and optoelectronics, a three-step sol-gel procedure was developed [38]. Additionally, ceramic films generated from sol-gel are also presented in [21]. Here are some further important papers on the sol-gel technique [39, 40, 41, 42, 43, 44, 45, 46, 47, 48].

Silica, titania, and silica-titania materials produced by the sol-gel technique have all undergone extensive research due to their potential optical uses [49, 50, 51, 52, 53, 54]. The early part of the 1980s saw the beginning of their use in the production of silica-titania WG films. The first individuals to do so were Herrmann and Wildman. However, they used MERCK's [50] commercially available liquid-coat solutions rather than synthetic sols. The research team led by W. Lukosz produced planar evanescent WG chemical/biochemical sensors utilizing these WG films, which were coated on glass substrates using the dip-coating technique and had refractive $n=1.8$ at $\lambda=612.5 \mu\text{m}$ [51, 55, 52, 53]. These films have optical losses of 2.5 dB/cm for $\lambda=632.8 \mu\text{m}$ [55]. Spin-coating was used by Jiwei et al. to fabricate $\text{SiO}_2\text{-TiO}_2$ WG films that were then coated on SiO_2/Si (111) substrates [54]. The greatest refractive index of the films was $n=1.87$ at $\lambda= 632.8 \mu\text{m}$, yet they had very significant optical losses of 7.4 dB/cm . It should be noted that 750°C annealing temperatures were used to generate such a high refractive index value. The phase change from

anatase to rutile is expected to occur at such high temperatures, making WG films much lossy. There are also other studies [56, 57, 58, 59] reporting the creation and characterization of composite $\text{SiO}_2\text{-TiO}_2$ films, although their waveguiding characteristics were not studied.

If the titania concentration is greater than 20% wt, the sol-gel-based manufacturing process of $\text{SiO}_2\text{-TiO}_2$ is quite challenging. This is due to titania's great propensity to crystallize and produce distinct phases. As a result, manufactured films exhibit large optical losses and are not amorphous [60]. Another issue that causes optical losses to increase over time is long-term stability [61]. These challenges were overcome by Karasinski et al. by creating $\text{SiO}_2\text{-TiO}_2$ WG films with a 50% weight TiO_2 content that are low-loss and long-term stable [62]. Using the dip-coating process on BK7 glass substrates, silica-titanium WG layers with a $\text{SiO}_2\text{-TiO}_2$ =1:1 molar ratio were created, which were subsequently heated to 500 °C. The primary chemical precursors for silica SiO_2 and titania TiO_2 are tetraethyl orthosilicate $\text{Si}(\text{OC}_2\text{H}_5)_4$ (TEOS) and tetraethyl orthotitanate $\text{Ti}(\text{OC}_2\text{H}_5)_4$ (TET), respectively. Water, ethanol, and hydrochloric acid (HCl), which catalyzes the processes of condensation and hydrolysis, are the additional substances used in the procedure.

Nanoimprint lithography (NIL) is used to construct a Bragg grating (BG) device in a sol-gel silica WG for bio-photonic applications [63]. A reasonably wide area in the range of several micrometers with a resolution in the order of several nanometers is achieved by the procedure, which also achieves non-standardized lithography in sol-gel silica at a high resolution. In a sol-gel silica optical WG, structures with 250 and 90 nm resolutions were shown for a sizable area that has not yet been tuned. For a 1 mm long region, a 250 nm periodic structure BG is produced. Two sol-gel silica BG structures, one measuring 250 nm broad and the other 90 nm wide, were then photographed using SEM as shown in **Figure 3** (a,b). The transmission and reflection spectrum of the BG structure is presented in **Figure 3** (c) and **Figure 3** (d), respectively. Based on the transmission and reflection spectra of laser light coupled into the WG at a wavelength of 1.55 μm , the efficiency of the grating structure in the WG was evaluated. The transmission and reflection spectra demonstrate that the WG grating was successfully constructed using the NIL procedure.

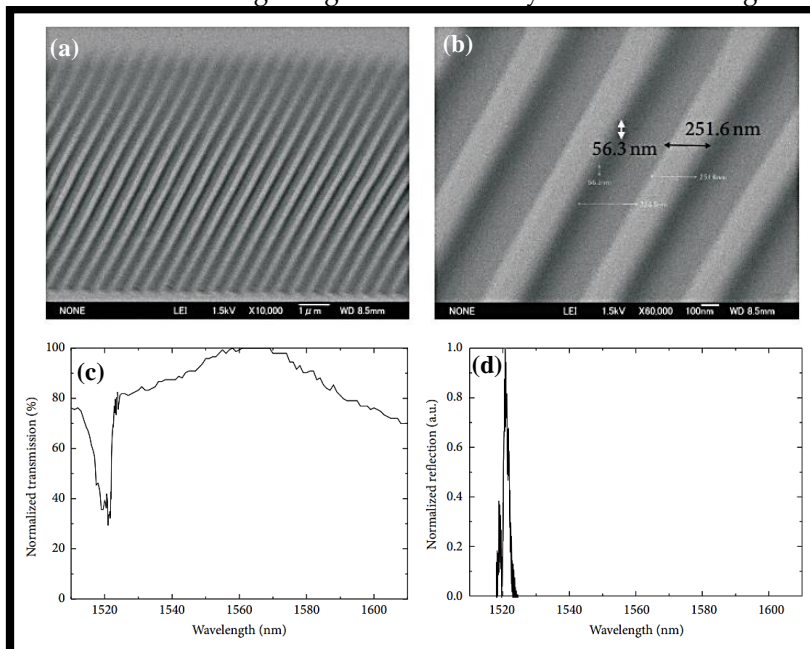


Figure 3. Sol-gel silica BG, (a) SEM image of the large area of periodic structure [63], (b) Zoomed area of the periodic structure [63], (c) transmission spectrum of the BG structure [63], (d) reflection spectrum of the BG structure [63].

3. Spin-coating

Spin-coating is a common technique for producing uniform coatings of the necessary thickness; unfortunately, because spin-coating wastes resources at a rate of more than

90%, materials prices increase as the film-coated area grows [64]. Since many years ago, thin films have been deposited via spin-coating. In this method, a tiny drop of coating material is put into the substrate's center before the substrate is rotated at a regulated high speed. The substrate spins during the spin-coating process around an axis that must be parallel to the region to be coated. Consequently, a thin coating film forms on the surface as the coating material distributes toward and finally moves away from the substrate's edge. The kind of coating (viscosity, drying rate, % solids, surface tension, etc.) and the spin processing conditions, such as rotation speed, will determine the final film thickness and other attributes. The stages of the spin-coating process are shown in **Figure 4**. The size of the substrate is one of the key drawbacks of spin-coating. High-speed spinning is more challenging as the size goes up since film thinning gets more challenging. There is practically limited material efficiency in spin-coating. In general, throughout the process, 95 to 98 % of the material is thrown off and discarded, and only 2 to 5 % of the material is dispensed onto the substrate.

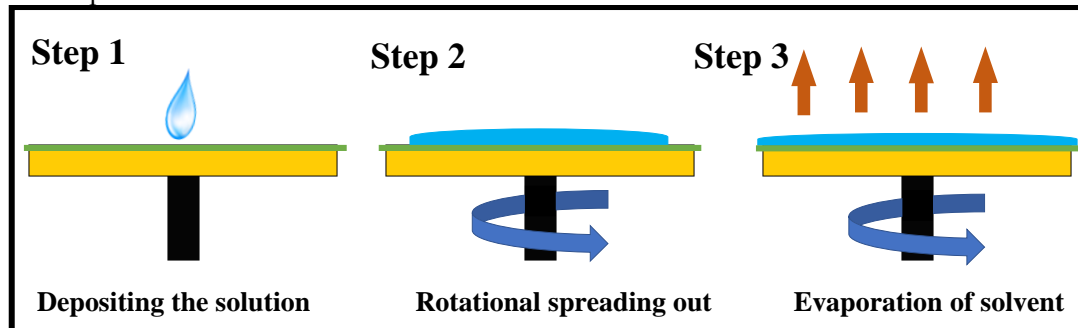


Figure 4. Stages of spin-coating of thin-film on a substrate.

To change the solid loading, viscosity, and volatility of the coating solution using this approach, several organic additives are frequently used. This technique is very well adapted to create an ultrathin film on different substrates. In 1958, Emslie and colleagues suggested the spin-coating process model forecast the film thickness as a function of specific physical parameters. The dip-coating parameters can be correlated using this method, though [65]. Huang and Chou further claimed, based on this function, that the solution's viscosity greatly depends on the shear rate because viscosity is linked to the shear stress. Theoretically, the shear forces caused by viscosity and solution spinning mostly influence the membrane thickness. A thinner, yet more homogeneous membrane would be produced by the spin-coating process' less viscous precursor solution [66]. Burmann et al. showed that while the solvent evaporation effect is important when employing the spin-coating for membrane casting, the rotational duration had little impact on membrane thickness. Nevertheless, the quick solvent evaporation might result in membranes that are unreliable and fragile [67]. Self-supporting ultrathin TiO_2 films were disclosed by Hashizume and Kunitake using the spin-coating method [68]. The spin-coating method was used to create the ultrathin layer of polyvinyl alcohol (PVA), which was then coated with titanium tetrabutoxide. The self-supporting ultrathin PVA/titanium composite film was eventually created by dissolving the soluble polymer. Spin-coating is frequently employed in labs to create small-sized membranes, but the technique is not appropriate for producing photocatalytic membranes on a large scale to be used in practical applications.

Due to defects in the thin films that make up organic solar cells, they are typically not repeatable. Wet spun-on PEDOT:PSS films are subjected to an imposed ultrasonic substrate vibration post-treatment to reduce the density of pinholes and defects in PEDOT:PSS, which is the hole transporting layer of a standard polymer solar cell, consisting of glass/ITO/PEDOT:PSS/P3HT:PCBM/Al, and to reduce scattering in device performance (SVPT) [69]. The forced vibration enhances the wet spun-on films' mixing and homogeneity, which in turn improves the nanostructure of the resulting thin solid films. The average power conversion efficiency of 14 identical cells rises by 25% when the SVPT, a mechanical, one-step, and low-cost technique, is used, and the standard deviation drops by 22%, showing that the device's photovoltaic performance is greatly enhanced and becomes

more consistent. This does away with various time-consuming, costly chemical and thermal processes that are typically used to increase cell repeatability [69]. The schematic of the whole device and a cross section of a cell that was photographed using a SEM are shown in **Figure 5 (a,b)**. The cross-sectional SEM picture in **Figure 5b** shows that the PEDOT: PSS film has a thickness of roughly 40 nm when the spin rotation is adjusted to 5000 rpm. It is calculated that the PEDOT: PSS film thickness produced at 3000 and 4000 rpm is 52 and 45 nm, respectively. The film was dried at 120°C for 30 minutes after the PEDOT: PSS solution was deposited, whether with or without ultrasonic vibrations [69].

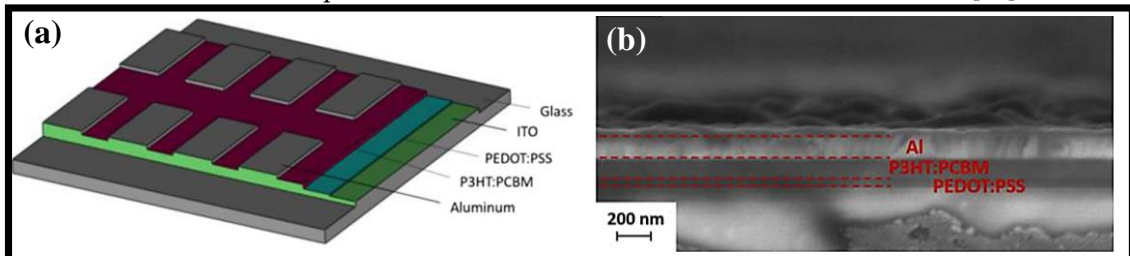


Figure 5. Graphical illustration of the solar cell [69], (b) SEM cross-sectional image of a cell [69].

4. Roll-coating

Roll-coating is a pre-metered coating that applies coating liquid to a substrate using a succession of rollers. The amount of coating material provided to the substrate is practically independent of the characteristics and structures of the fabric because a metered layer of the coating liquid is first generated on the roller surface before it is transferred to the substrate. Precise control is achievable and is mainly governed by the rheology of the fluid and the relative speed of two spinning surfaces. A single revolving roller is used in the most basic roll-coating setup. The roller's upper portion is in touch with the substrate, while its lower half is submerged in a coating liquid bath. A portion of the liquid film formed by the coating liquid on the roller surface is transferred from the roller surface to a substrate as the roller rotates. Hydrodynamics controls the quantity of coating that is applied to the substrate. The elements affecting coating thickness include substrate speed, roller rotation speed, and rheological characteristics of the coating fluid. One roller serves as both metering and an application device in this configuration. By adding additional rollers, more accurate control is made possible.

A metering roller, an applicator roller, and a backup roller are all used in a three-roll coating. Nip feed coating and L-head coating are typical three-roll arrangements. In three-roll nip feed coating, the nip created by a metering roller and an applicator roller serves as a reservoir and is inundated with coating liquid. The metering roller rotates in the opposite direction to the applicator roller and measures the amount of coating liquid transferred to the substrate once the applicator roller picks up the coating liquid from the nip. Any coating liquid that remains on the metering roller surface after the coating liquid passes from the metering roller to the applicator roller is cleaned with a doctor blade to prevent coating defects like streaks or rough film. A backup roller supports the film as it is deposited onto the substrate surface from the applicator roller. Although this design only requires a little amount of coating fluid, it tends to leak. When coating liquid has a low viscosity, it might be difficult. A liquid film is created on the applicator/dipping roller revolving through the coating liquid in a three-roll pan feed or L-head coating, metered by a metering roller, and coated on the substrate fabric on a backup roller as shown in **Figure 6**.

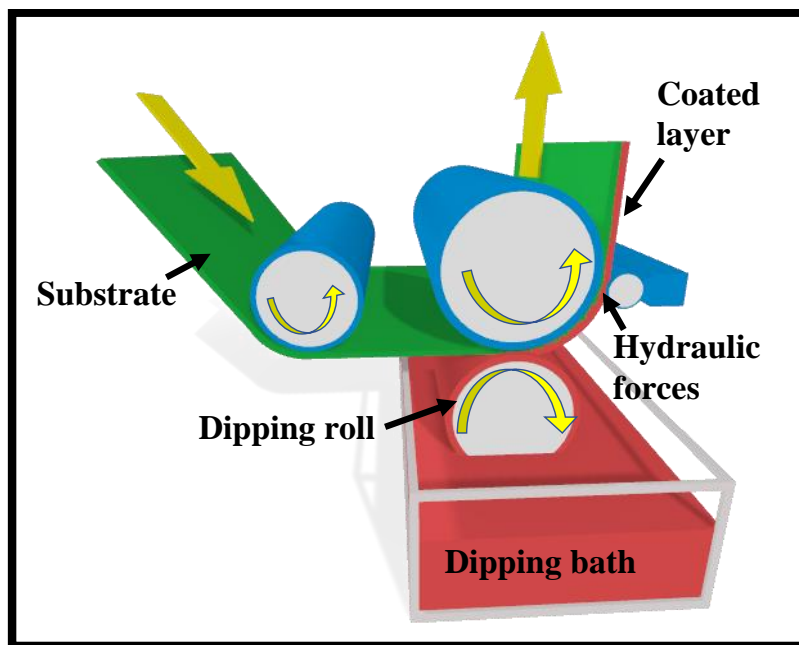


Figure 6. Roll-coating set-up.

A fourth roller—a pick-up roller operating at a slower speed—can be installed to boost coating speed. This method is known as a four-roll pan-fed coating system. Since the applicator and metering rollers rotate in opposite directions, the configurations in Figure are referred to as reverse metering. Forward metering is the term used when they both rotate in the same direction. Forward roll metering usually produces unstable, non-uniform films, whereas reverse metering generates smoother, more stable films. As a result, reverse roll coating is increasingly frequently employed. Hot melts, solvent-based coatings, and water-based solutions can all be used for roller coating. Hot melt roller coating involves melting solid pellets between hot melt rollers, creating a melt film, then depositing the melt film on a substrate. Typically, hot melt is applied after preheating the substrate.

Under the presumption of a small roll curvature, Greener and Middleman did the theoretical study on roll-coating and examined the scenario where the roll and sheet are moving at the same speed [12]. They were able to determine the precise equation for film thickness and pressure distribution for a Newtonian fluid under the approximation of lubrication. They quantitatively calculated film thickness, pressure, and roll-separating force for viscoelastic and power-law fluids as well. The overall Navier-Stokes equations were solved by the finite element method by Coyle et al. [70]. They then examined the approximated lubrication model's findings and concluded that it was effective only for systems with large capillary numbers and low surface tension. Hintermaier and White used a lubricating scheme to study the flow of water between two rollers, and their calculated techniques closely matched their reported performance [71]. The coating fluxes for several non-Newtonian fluid models were both theoretically and empirically investigated by Benkreira et al. [72, 73, 74, 75]. Sofou and Missoula used the power lubrication theory, Bingham plastics, and Hershel-Bulkley models to examine the roll-over-web coating flow computationally [76].

Utilizing a third-grade fluid lubrication approximation, Zahid et al. examined the roll coating process and numerically evaluated all the crucial characteristics. By assuming that both the roller and the sheet are porous [77]. They also theoretically explored the second-grade fluid roll coating method [78]. It is expected that the pace at which fluid enters the roller surface will be the same as the rate at which fluid exits the web surface. With the support of the lubrication approximation theory, Ali et al. investigated the web-coating method for a pair stress fluid [79]. They also evaluated the pressure gradient, pressure, velocity, roll-separating force, power input, and other crucial parameters. By bringing the pair stress constant to infinity, the findings were compared to those from the Newtonian

fluid. To conduct an experimental investigation of the forward and reverse roll-coating processes in meniscus fluid mechanics, Gaskell et al. adopted an optical sectioning technique [80]. To determine key parameters such as intake flow rate, film thickness, meniscus position, and pressure field, several tests were carried out. Nevertheless, the optimal homotopy asymptotic method (OHAM) was not used to assess the impacts of pair stresses generated during the roll-over-web operation. A semi-analytical approximation method for solving non-linear problems is the OHAM [81]. In contrast to other methods of perturbation, this methodology is independent of any big or small factors and offers a suitable way to manage the convergence of the approximation solution and, if necessary, modify the convergence zones.

5. Spray-coating

Considering the abundance of paints and varnishes included in spray devices that can be purchased in stores all over the world, the spray-coating technique may be one of the most useful for covering surfaces. It might be difficult, though, to find a sprayer and coating solution that work well together. There are also other variants of this procedure, including spray-coating with plasma [82], thermal spray [83], and powder [84], among others. The traditional spray-coating method is still the most often reported due to its low cost and lack of specialized equipment, though. Some equipment is connected to compressors for photocatalytic coating so that the solution exits at the desired speed and pressure [85]. Similar to the dip-coating technique, the solution must be correctly prepared before being loaded into the spray. The precursor solution employed by Montecchio et al. contained merely commercial TiO_2 and ethanol at a ratio of 1:20 by mass, respectively, and produced promising benefits after being applied to both steel and ceramic plates on several occasions [86]. Following the structure's preparation or pretreatment, the coating is carried out using a spray, and the material is then allowed to dry at a specified temperature and time. To get the appropriate thickness or catalyst mass, the technique can be done numerous times. **Figure 7** is a schematic illustration of the spray-coating method. Zinc acetate dihydrate and methanol were used in an ultrasonic spray pyrolysis process by Bousmaha et al. to coat ZnO in a glass tube [87]. The methylene blue dye completely degraded during photocatalytic experiments, and the scientists claim that this method is the best for creating thin layers on flat surfaces like glass.

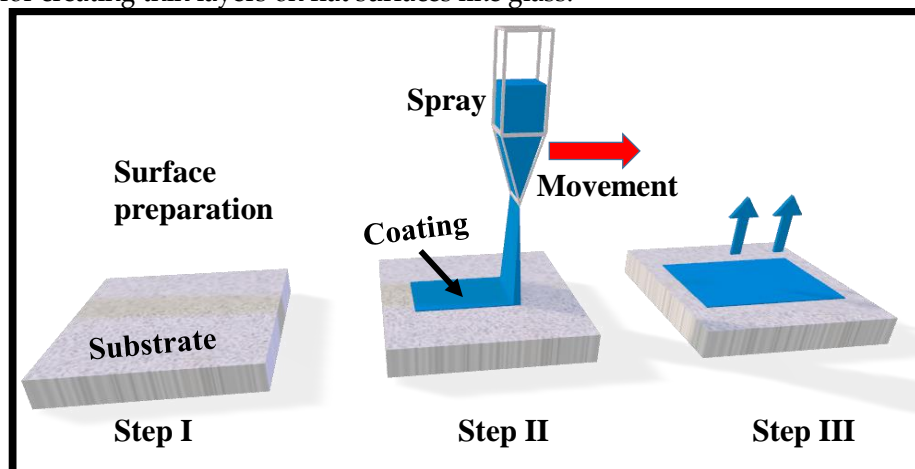


Figure 7. Spray coating process.

A fine aerosol is created by forcing printing ink through a nozzle during the spray-painting process. PSC's typical performance in a spray coating method is constrained by issues including isolated droplets, a non-uniform surface, and pinholes. The distance between the sample and the airbrush, the flow rate, the pressure, the substrate temperature, the concentration of the blend solution, the duration of the spray, the cosolvent mixture, and the number of times the substrate is sprayed are just a few of the process variables for spray coating that have been extensively studied.

With a cell size of 2.5 cm², the greatest PCE observed is 4.1 percent. The polymer active layer was prepared using mixed solvents, and the substrate was also heated to 40 °C. It has been shown that decreasing PCE results in scaling up the cell area [88]. According to research by Park et al. [89] and Kang et al. [17], the PCE of the devices decreased as the cell area increased. The high sheet resistance of the transparent electrode and the challenging tuning of the large-area deposition process are to blame for this.

In studies on photoelectric devices, the ultrasonic spray coating process (USCP) has proven appealing due to its high material efficiency, cheap manufacturing costs, and suitability to simplify production. Surface tension in the solvent, though, continues to be a major barrier to USCP's ability to produce a smooth organic layer for OLEDs. By integrating an extra-low surface tension diluent and a surface tension control mechanism, a high-quality polymer anode buffer layer and tiny molecule emission layer are effectively achieved by USCP [90]. Poly (3,4-ethylene dioxythiophene) polystyrene sulfonate (PEDOT: PSS) films benefit from the addition of low surface tension methyl alcohol because it causes clear phase separation and increases conductivity. Additionally, a surface tension control technique is provided to remove the influence of surface tension during the solvent evaporation stage of ultrasonic spray coating the film.

A two-step sequential deposition method is used to construct methylammonium lead iodide perovskite solar cells using simple coating processes like spray coating and drop-casting [91]. In the first stage, spray coating replaces the often-used lab-scale spin-coating for the deposition of the lead iodide, while the operating parameters of the former process are improved to produce a completely coated and homogeneous sheet of lead iodide. In the second phase, the touch-free drop-casting and scalable pulsed-spray coating substitute the dip-coating procedure to deposit methylammonium iodide on top of the lead iodide layer to create methylammonium lead iodide perovskite. It has been discovered that the efficiency of perovskite films and devices created using pulsed-spray coating and drop-casting is comparable to those created using dip-coating and that these methods, along with drop casting's low material requirements, have the potential to take the place of dip-coating in the production of perovskite solar cells on a large scale. Spray-drop and spin-drop processes were used to create the winning devices, which showed power conversion efficiencies of 6.92 percent and 9.48 percent, respectively. Higher efficiencies are anticipated because of applying the improved characteristics and additional layers when fabricating devices in a low-humidity environment [91].

The typical constructed devices' SEM cross-sectional images without the rear contact are shown in **Figures 8(a)** and **Figure 8(b)**. The photos demonstrate the formation of a thin, homogeneous layer of spun-on c-TiO₂ that is less than 100 nm thick. When compared to perovskite films created with spin-drop coating, spray-drop films are thicker and less homogeneous. **Figure 8(c)** displays the characteristics of the current density and voltage. The array of spray-drop devices with a 9 mm² cell size is seen in the inset image of Figure X(c) on a single substrate. Additionally, the average PCE from spin-drop cells (8.45%) is greater than the average for spray-drop cells (5.95 percent).

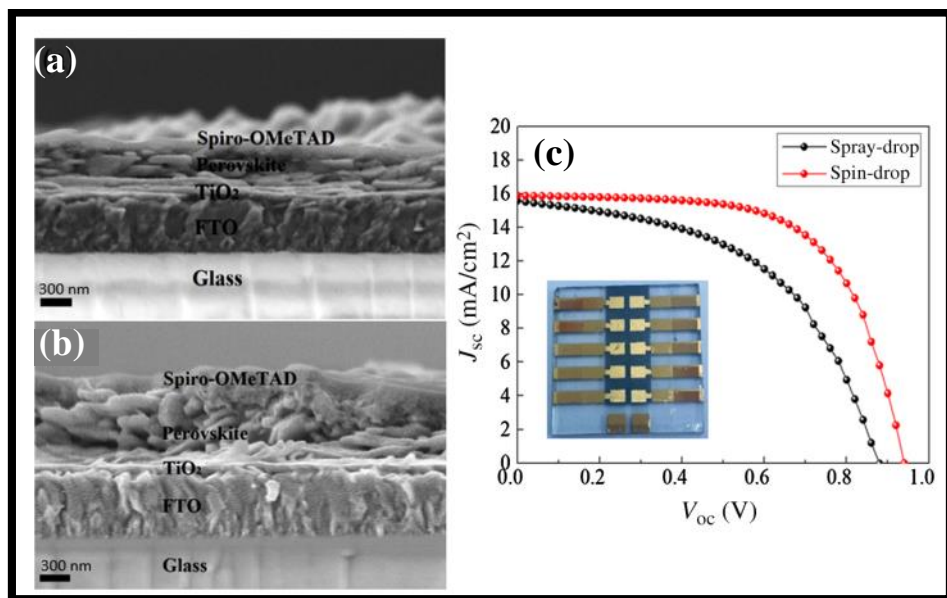


Figure 8. SEM cross-sectional images of planar PVSCs made by (a) spin-drop, (b) spray-drop coating without a back contact [91]. (c) J-V curves, where the spin-drop and spray-drop coating processes are used to create the perovskite layer. The instrument constructed using the spray-drop approach is seen in the inset [91].

6. Blade-coating

The production of each layer of the PSC using scalable coating technique and the development of high-performance devices across a vast area are two of the main obstacles to the effective commercialization of perovskite photovoltaics. The perovskite layer used in today's most effective PSCs is currently made via spin-coating and anti-solvent dripping to produce dense, pinhole-free layers with good optoelectronic quality [92, 93, 94, 95]. Due to the substantial solution waste generated by spin-coating—up to 90% of the dripping solution might be expelled during spinning [96]—it is not a cost-effective process. Additionally, spin-coating does not produce films that are consistent from corner to corner, which emphasizes large-area substrates ($>10\text{ cm} \times 10\text{ cm}$). In the end, spin-coating is not appropriate for continuous roll-to-roll (R2R) high throughput manufacturing operations and big area in-line processes. To scale up perovskite photovoltaics, it is desirable to create alternative scalable deposition techniques [97].

Uniform perovskite films may now be deposited on large-area surfaces using a variety of industrially scalable deposition techniques that are suitable for high throughput manufacturing. These scalable deposition techniques may often be separated into the solution- and vapor-based processes. Blade-coating [98, 99], slot-die-coating [100], inkjet printing [101], and spray-coating [102] are examples of solution-based techniques that allow you to incorporate additives into the precursor solution to regulate film production and improve morphology.

Blade coating offers the benefit of large-area homogeneity, little material waste, interlayer dissolution prevention, compatibility with roll-to-roll manufacturing, and more efficient use of active material while still allowing for the preparation of well-defined films [103]. The blade coating method's quick-drying step avoids the traditional solvent annealing procedure from slowing down manufacturing throughput [104]. The schematic of the blade-coating method is shown in **Figure 9**. By altering the fabrication conditions, such as the solution concentration, the blade gap, and the blade coating speed in this process, the film thickness may be adjusted. Using blade coating techniques, PSC based on PBDTTT-C-T: PCBM was demonstrated which performed well with the chlorine-free solvents toluene and xylene [104]. The superior solubility of PBDTTTC-T in the chlorine-free solvents is the primary factor contributing to the increase in PSC performance. Additionally, the blade-coated film had smoother surfaces than spin-coated film, which somewhat raised the power conversion efficiency (PCE) of the blade coated PSC.

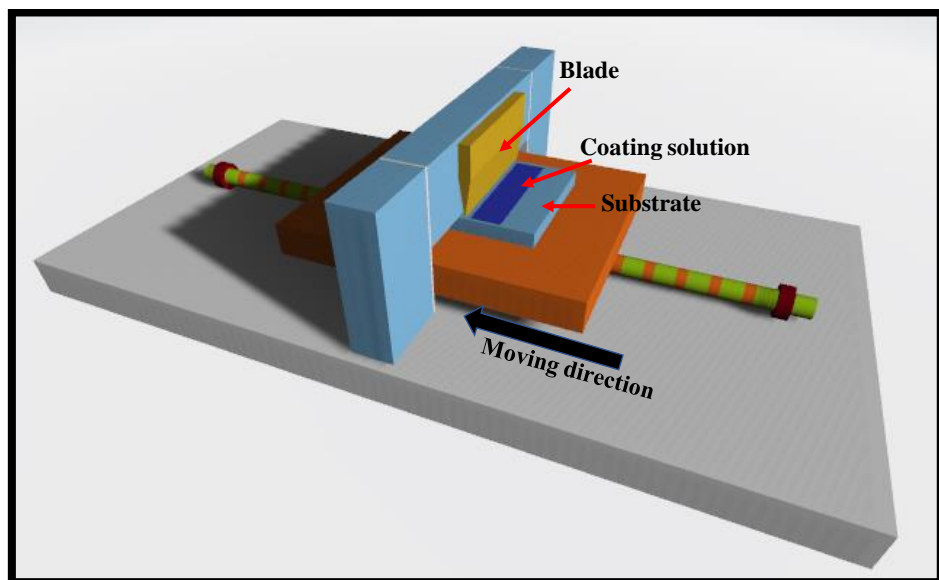


Figure 9. Blade coating setup.

When P3HT: PCBM PSC was manufactured using several coating processes, including spin-coating, blade coating, blade coating on a hotplate, as well as blade and spin-coating, the same effect was seen [105]. Because the polymer chains are comparatively able to move freely in the absence of centrifugal force, the polymer films produced by blade coating with toluene, a chlorine-free solvent, were more structured than those produced by spin-coating. Therefore, it can be said that such approaches provide the necessary ordered and interpenetrating morphology in polymer films without the requirement for any post-production treatment, such as solvent annealing and heat annealing.

One of the main difficulties in producing highly efficient organic-inorganic PSCs is scaling them up. On large-area substrates, uniform perovskite films of good crystal quality have been sought after using a variety of scalable techniques, but each of these techniques has its constraints on the possibility of perovskite photovoltaics' effective commercialization. Here, a completely scalable hybrid approach is illustrated that combines vapor- and solution-based methods to produce homogeneous perovskite films of excellent quality on surfaces with vast surface areas [106]. This two-step procedure avoids the use of hazardous solvents and makes it simple to include passivation techniques and additives. This technology is used to manufacture PSCs that employ blade coating to deposit SnO_2 electron transporting layers and Spiro-OMeTAD hole transporting layers in ambient air without the need for halogenated solvents. On substrates measuring 5 cm by 5 cm, the manufactured PSCs attained an open-circuit voltage of up to 1.16 V and a power conversion efficiency of 18.7% with good uniformity [106].

The concept for the scalable PVD/blade coating technique to create the perovskite layer is shown in **Figure 10 (a)** [106]. The three phases that make up this hybrid technique. The inorganic halide template is first consecutively formed by thermal evaporation on substrates coated in transparent conducting oxide with an electron transporting layer (SnO_2). The layers in this template are 15 nm thick cesium iodide (CsI) on bottom of a 300 nm thick lead iodide (PbI_2) layer. The second stage involves blade coating the inorganic halide template with the organic halide precursor solution, which is made up of formamidinium iodide (FAI), methylammonium bromide (MABr), and methylammonium chloride (MACl) mixed in isopropanol. To encourage crystal development, lessen grain boundaries, and produce a compact perovskite film with large grain size, thermal annealing at 150 °C for 15 min in ambient air is done as the last step. SEM pictures of the film morphology at each stage of the PVD/blade coating process are shown in **Figures 10(b–g)** [106].

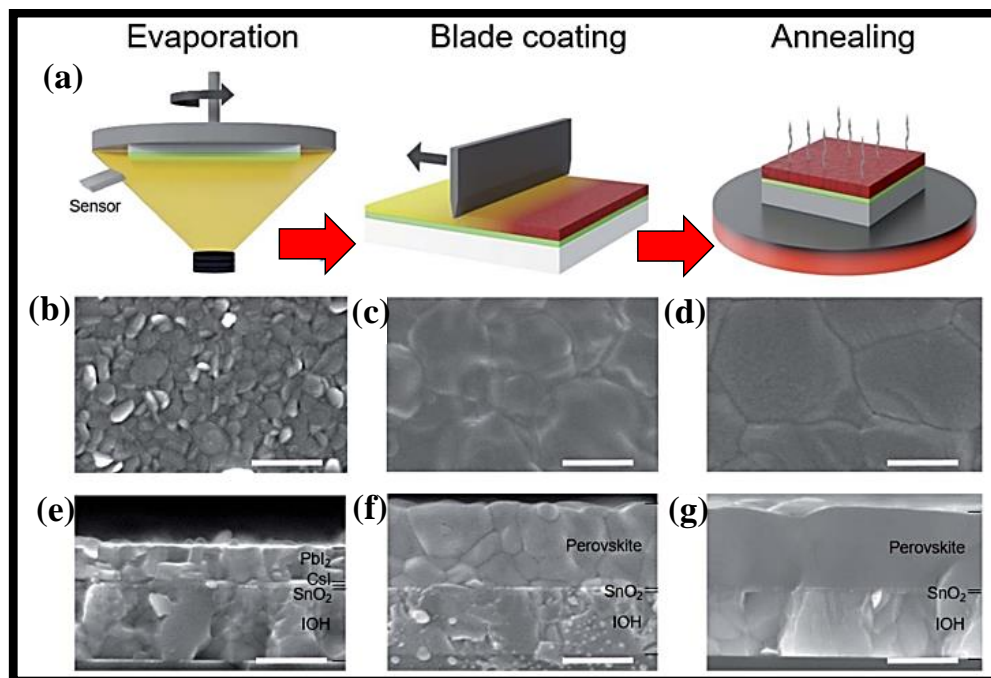


Figure 10. Perovskite layers and structure following each phase of the hybrid PVD/blade coating technique [106]. (a) A flowchart showing the three stages involved in fabricating a PVD/blade coating. Following each phase of manufacturing, SEM top and cross-section view images are shown in (b) and (e) after evaporation, (c) and (f) after blade coating, and (d) and (g) after thermal annealing [106].

7. Other thin-film deposition methods

Over the past 20 years, a variety of physical and chemical deposition techniques have been employed to produce nanostructured thin films [107, 108]. Both strategies provide certain advantages over more conventional methods and have a bright future in the deposition process. New transparent materials must be deposited at low temperatures on conducting and non-conductive substrates to use thin-film technology.

Physical vapor deposition (PVD) techniques include thermal evaporation [109], electron beam [110], pulsed laser [111], molecular beam epitaxy [112], ion plating [113], and activated reactive evaporation [114]. The goal of this deposition technique is to transfer atoms from a source to a substrate such that independent film formation and growth may take place. There are several drawbacks, too, such as the requirement for a pricey vacuum environment and expensive instrumentation. The vaporization coating method known as PVD calls for an atomic-level material transfer. This vacuum-based process transfers vaporized material from a source to a substrate, where it condenses after passing through a vacuum or low-pressure gas environment.

The ability to rotate different source materials into the path of the electron, which prevents the vacuum from being disrupted, is one advantage of E-Beam Evaporation. E-beam evaporation is widely used for optical thin-film applications, including laser optics, solar panels, eyeglasses, and architectural glass. A broad variety of materials are deposited using this method. It provides the essential mechanical, electrical, and optical qualities. E-beam evaporation offers a high material utilization efficacy compared to other PVD processes, reducing the cost of production.

Chemical vapor deposition (CVD) is a kind of deposition that creates high-performance solid materials, often in a vacuum. The nonvolatile solid thin films that are formed on substrates in this method are created by chemical reactions involving organometallic or halide chemicals and other gases. The primary distinction between this approach and PVD is the direction of material deposition on the substrate; PVD is a line-of-site impingement. To deposit materials in a variety of morphologies, including epitaxial, amorphous, monocrystalline, and polycrystalline, CVD is frequently employed in microfabrication techniques. Contrary to PVD, a solid coating is established on the surface of the substrate

because of a chemical interaction between a mixture of gases and the bulk surface of the material in CVD. This chemical reaction also allows for the chemical degradation of some of the gas's components. Additionally, numerous cutting-edge CVD systems and their alternatives, such as plasma-enhanced CVD (PECVD) [115] and metal-organic CVD (MOCVD) [116], have been commercialized. This enables the structures and characteristics of the resultant products to be modified. Typically, CVD does not need high-vacuum working settings, making it a popular technology for electronics, optoelectronics, and biomedical applications. Numerous papers describe the deposition of high-quality waveguide films using CVD or its substitutes [117, 118, 119].

Research is being done on a technique called spray pyrolysis for producing thin and thick films, ceramic coatings, and powders [120]. It stands out as a highly straightforward and rather cost-effective processing approach, especially when it comes to equipment expenses, compared to many other film deposition procedures. This technique involves spraying a solution onto a heated surface, where it reacts to generate a chemical compound, depositing a thin coating [98]. Chemical reactants are designed so that at the deposition temperature, products other than the necessary components are volatile. It offers an exceedingly straightforward method for creating films of any composition. This technique has been utilized by researchers to create premium thin films that may be used in a variety of optical components [121, 122, 123, 124].

8. Author's opinion on coating methods and concluding remarks

Along with the material to be utilized as a framework for photocatalysts, the coating technique must be appropriate and well-planned. Given the seriousness, thermal treatments or methods of acidic solution deposition can destroy the material's structure. For instance, unlike glass and metals, polymers cannot resist high temperatures. As a result, the approach must be appropriate for specific applications. Dip-coating, spray-coating, electrolytic deposition, and thermal attack are the coating methods that have been utilized most often lately. Other methods including doctor blades, spin-coatings, and paint-based coatings have also been documented, albeit less often. It is also possible to find modifications of these methods, always attempting to adapt to the coating structure and material type deposition.

In both industrial settings and research labs, spin-coating, dip-coating, and spray-coating are particularly popular methods for depositing thin films. Due to its great repeatability and adaptability across a broad viscosity range, spin-coating is one of the crucial routes for lab scale. It is a rapid and simple method to build homogenous film at a tiny scale, ranging in thickness from a few nanometers to a few micrometers. Due to its high material consumption and confinement to a broad region, it is not suited for industrial scale-up. Since dip-coating can easily and quickly deposit thin films over a broad area, it is frequently used for mirror coating and dye processing. The dip-coating method has the great ability to be able to coat structures with geometries that have concealed faces or tight corners, but there is a significant loss of precursor solution during the procedure because the container used must hold enough solution to surround the structure during immersion. The main benefits are the ability to process a big area and the ability to adjust film thickness by withdrawal speed and solution viscosity. Large tanks and a lot of coating solutions are needed for dip-coating. Even though the solution has a lengthy deposition life (a few months), only approximately 20% of it can be utilized.

The spray-coating method allows the flexibility to adjust the system to apply any sort of solution and achieve the appropriate film thickness. It has access to a wide range of fluids. It has a significant potential for mass manufacturing and is repeatable. The spray-coating approach can be applied fast if it has appropriate spray apparatus, but it is not suitable for irregular geometries with concealed faces. Doctor blading is a method that works well for coatings that are applied on a wide scale. The method may also be used to make thicker films out of a viscous solution. It cannot provide homogeneity at the nanoscale or the very thin sheets that spin-coating can.

Author Contributions: Conceptualization, M.A.B.; software, M.A.B.; validation, M.A.B.; formal analysis, M.A.B.; investigation, M.A.B.; resources, M.A.B.; data curation, M.A.B.; writing—original draft preparation, M.A.B.; writing—review and editing, M.A.B.; visualization, M.A.B.; supervision, M.A.B.; project administration, M.A.B.; funding acquisition, M.A.B.

Funding: The research is co-financed by the Foundation for Polish Science from the European Regional Development Fund within the project POIR.04.04.00-00-14D6/18 "Hybrid sensor platforms for integrated photonic systems based on ceramic and polymer materials (HYPHa)" (TEAM-NET program).

Institutional Review Board Statement: Not applicable.

Informed Consent Statement: Not applicable.

Data Availability Statement: Not applicable.

Acknowledgments: The author acknowledge the active contribution of a young researcher Ms. Alsu Shakmaeva in the preparation of high-quality images used in this manuscript.

Conflicts of Interest: The authors declare no conflict of interest."

References

- [1] S. Weinstein and K. Ruschak, "Coating flows," *Annual Review of Fluid Mechanics*, vol. 36, pp. 29-53, 2004.
- [2] F. Krebs, "Fabrication and processing of polymer solar cells: A review of printing and coating techniques," *Solar Energy Materials and Solar Cells*, vol. 93, no. 4, pp. 394-412, 2009.
- [3] R. Konar and G. Nessim, "A mini-review focusing on ambient-pressure chemical vapor deposition (AP-CVD) based synthesis of layered transition metal selenides for energy storage applications," *Materials Advances*, vol. 3, no. 11, pp. 4471-4488, 2022.
- [4] S. Rossnagel, "Thin film deposition with physical vapor deposition and related technologies," *Journal of Vacuum Science & Technology A*, vol. 21, p. S74, 2003.
- [5] R. Johnson, A. Hultqvist and S. Bent, "A brief review of atomic layer deposition: from fundamentals to applications," *Materialstoday*, vol. 17, no. 5, pp. 236-246, 2014.
- [6] Y.-S. Hong, S.-R. Lee, J.-H. Kim and S.-Y. Lee, "Application of a DLC-coating for improving hydrostatic piston shoe bearing performance under mixed friction conditions," *Int. J. Precis. Eng. Manuf.*, vol. 16, no. 2, pp. 335-341, 2015.
- [7] P. Tandon and H. Boek, "Experimental and theoretical studies of flame hydrolysis deposition process for making glasses for optical planar devices," *Journal of Non-Crystalline Solids*, vol. 317, no. 3, pp. 275-289, 2003.
- [8] J. M. Ruano, V. Benoit, J. S. Aitchison and J. M. Cooper, "Flame hydrolysis deposition of glass on silicon for the integration of optical and microfluidic devices," *Anal. Chem.*, vol. 72, no. 5, pp. 1093-1097, 2000.
- [9] Y. Yang, K.-H. Kim and J. Ong, "A review on calcium phosphate coatings produced using a sputtering process: An alternative to plasma spraying," *Biomaterials*, vol. 26, no. 3, pp. 327-337, 2005.
- [10] Butt, M. A; et al., "Fabrication of Y-splitters and Mach-Zehnder structures on (Yb, Nb):RbTiOPO4/RbTiOPO4 epitaxial layers by reactive ion etching," *Journal of Lightwave Technology*, vol. 33, no. 9, pp. 1863-1871, 2015.
- [11] M. A. Butt, E. S. Kozlova and S. N. Khonina, "Conditions of a single-mode rib channel waveguide based on dielectric TiO2/SiO2," *Computer Optics*, vol. 41, no. 4, pp. 494-498, 2017.
- [12] S. Middleman, *Fundamentals of polymer processing*, New York, NY, USA: McGraw-Hill, 1977.
- [13] R. Bird, G. Dai and B. Yarusso, "The rheology and flow of viscoplastic materials," *Rev. Chem. Eng.*, vol. 1, pp. 1-70, 1983.

- [14] J. Jeong, J. Lee, H. Kim, H.-K. Kim and S.-I. Na, "Ink-jet printed transparent electrode using nano-size indium tin oxide particles for organic photovoltaics," *Solar Energy Materials & Solar Cells*, vol. 94, pp. 1840-1844, 2010.
- [15] S. Eom, H. Park, S. Mujawar, S. Yoon, S.-S. Kim, S. Na, S.-J. Kang, D. Khim, D.-Y. Kim and S.-H. Lee, "High efficiency polymer solar cells via sequential inkjet-printing of PEDOT: PSS and P3HT: PCBM inks with additives," *Organic Electronics*, vol. 11, pp. 1516-1522, 2010.
- [16] M. Voigt, R. Mackenzie, S. King, C. Yau, P. Atienzar, J. Dane, P. Keivanidis, I. Zadrazil, D. Bradley and J. Nelson, "Gravure printing inverted organic solar cells: The influence of ink properties on film quality and device performance," *Solar Energy Materials & Solar Cells*, vol. 105, pp. 77-85, 2012.
- [17] J.-W. Kang, Y.-J. Kang, S. Jung, M. Song, D.-G. Kim, C. Kim and S. Kim, "Fully spray-coated inverted organic solar cells," *Solar Energy Materials & Solar Cells*, vol. 103, pp. 76-79, 2012.
- [18] C. Girotto, B. Rand, J. Genoe and P. Heremans, "Exploring spray coating as a deposition technique for the fabrication of solution-processed solar cells," *Solar Energy Materials & Solar Cells*, vol. 93, pp. 454-458, 2009.
- [19] R. Green and A. Morfa, "Performance of bulk heterojunction photovoltaic devices prepared by airbrush spray deposition," *Appl. Phys. Lett.*, vol. 92, p. 033301, 2008.
- [20] P. Karasinski, C. Tyszkiewicz, A. Domanowska, A. Michalewicz and J. Mazur, "Low loss, long time stable sol-gel derived silica-titania waveguide films," *Materials Letters*, vol. 143, pp. 5-7, 2015.
- [21] C. J. Brinker, G. C. Frye, A. J. Hurd and C. S. Ashley, "Fundamentals of sol-gel dip coating," *Thin Solid films*, vol. 201, no. 1, pp. 97-108, 1991.
- [22] Brinker, C. J.; et al., "Sol-gel derived ceramic films-fundamentals and applications," in *Stern K.H. (eds) Metallurgical and ceramic protective coatings*, Dordrecht, Springer, 1996.
- [23] J. Jaglarz, P. Dulian, P. Karasinski and P. Winkowski, "Scattering phenomena in porous Sol-gel-derived silica films," *Coatings*, vol. 10, no. 6, p. 509, 2020.
- [24] P. Karasinski, "Sol-gel derived optical waveguide films for planar sensors with phase modulation," *Opt. Appl.*, vol. 34, no. 4, pp. 467-475, 2004.
- [25] P. Karasinski, C. Tyszkiewicz and R. Rogozinski, "Rib waveguides based on the sol-gel derived SiO₂:TiO₂ films," *Photonics Letters of Poland*, vol. 2, no. 1, pp. 40-42, 2010.
- [26] T. Matsui, K. Komatsu, O. Sugihara and T. Kaino, "Simple process for fabricating a monolithic polymer optical waveguide," *Optics Letters*, vol. 30, no. 9, pp. 970-972, 2005.
- [27] A. Killinger, G. Gantenbein, S. Illy, T. Ruess, J. Weggen and V. Martinez-Garcia, "Plasma Spraying of a Microwave Absorber Coating for an RF Dummy Load," *Coatings*, vol. 11, no. 7, p. 801, 2021.
- [28] A. Hongo, M. Miyagi, Y. Kato, M. Suzumura, S. Kubota, Y. Wang and T. Shimomura, "Fabrication of dielectric-coated silver hollow glass waveguides for the infrared by liquid-flow coating method," in *Proceedings volume 2677, Biomedical Fiber Optics, Photonics West*, San Jose, CA, United States, 1996.
- [29] M. Faustini, B. Louis, P. Albouy, M. Kuemmel and D. Gross, "Preparation of Sol-Gel Films by Dip-Coating in Extreme Conditions," *J. Phys. Chem. C*, vol. 114, no. 17, pp. 7637-7645, 2010.
- [30] H. Hakki, S. Allahyari, N. Rahemi and M. Tasbihi, "Surface properties, adherence, and photocatalytic activity of sol-gel dip-coated TiO₂-ZnO films on glass plates," *Comptes Rendus Chim*, vol. 22, pp. 393-405, 2019.
- [31] D. Morais, R. Boaventura, F. Moreira and V. Vilar, "Advances in bromate reduction by heterogeneous photocatalysis: the use of a static mixer as photocatalyst support," *Appl Catal B Environ*, vol. 249, pp. 322-332, 2019.

- [32] A. Zarubica, "Modified nanostructured titania based thin films in photocatalysis: kinetic and mechanistic approach," *React Kinet Mech Catal*, vol. 115, pp. 159-174, 2015.
- [33] M. Butt, C. Tyszkiewicz, K. Wojtasik, P. Karasinski, A. Kazmierczak and R. Piramidowicz, "Subwavelength grating waveguide structures proposed on the low-cost silica-titania platform for optical filtering and refractive index sensing applications," *International Journal of Molecular Sciences*, vol. 23, p. 6614, 2022.
- [34] M. Butt, A. Kazmierczak, C. Tyszkiewicz, P. Karasinski and R. Piramidowicz, "Mode sensitivity exploration of silica-titania waveguide for refractive index sensing applications," *Sensors*, vol. 21, no. 22, p. 7452, 2021.
- [35] M. Butt, C. Tyszkiewicz, P. Karasinski, M. Zieba, D. Hlushchenko, T. Baraniecki, A. Kazmierczak, R. Piramidowicz, M. Guzik and A. Bachmatiuk, "Development of a low-cost silica-titania optical platform for integrated photonics applications," *Optics Express*, vol. 30, no. 13, p. 23678, 2022.
- [36] H. Schroeder, "Oxide layers deposited from organic solutions," in *Physics of thin films: Advances in Research and Developments*, New York & London, Academic Press, 1969, pp. 87-141.
- [37] S. M. Attia, J. Wang, G. Wu, J. Shen and M. A. Jianhua, "Review on sol-gel derived coatings: process, techniques and optical applications," *J. Mater. Sci. Technol.*, vol. 18, no. 3, pp. 211-217, 2002.
- [38] M. N. Logan, S. Prabakar and C. J. Brinker, "Sol-gel-derived silica films with tailored microstructures for applications requiring organic dyes," *MRS Online Proceedings Library*, vol. 346, pp. 115-120, 1994.
- [39] A. Fidalgo and L. M. Ilharco, "The defect structure of sol-gel-derived silica/polytetrahydrofuran hybrid films by FTIR," *Journal of Non-Crystalline Solids*, vol. 283, no. 1-3, pp. 144-154, 2001.
- [40] R. Parin, M. Rigon, S. Bortolin, A. Martucci and D. D. Col, "Optimization of hybrid sol-gel coating for dropwise condensation of pure steam," *Materials*, vol. 13, p. 878, 2020.
- [41] S. Acosta, A. Ayral, C. Guizard, C. Lecornec, G. Passemard and M. Moussavi, "Sol-gel derived silica layers for low-k dielectrics applications," *MRS online Proceedings Library*, vol. 612, p. 5261, 2000.
- [42] M. Boudot, V. Gaud, M. Louarn, M. Selmane and D. Grosso, "Sol-Gel based hydrophobic antireflective coatings on organic substrates: A detailed investigation of Ammonia Vapor Treatment (AVT)," *Chem. Mater.*, vol. 26, no. 5, pp. 1822-1833, 2014.
- [43] T. Kim and K. Song, "Low-temperature preparation of superhydrophilic coatings using tetraethoxysilane and colloidal silica by sol-gel method," *Colloids and Surfaces A: Physicochemical and Engineering Aspects*, vol. 647, p. 129105, 2022.
- [44] M. Hasaneen, M. Shalaby, N. Yousif, A. Diab and E. Agammy, "Structural and optical properties of transparent conducting oxide Cd_{1-x}Cr_xO thin films prepared by the sol-gel dip-coating method," *Materials Science and Engineering: B*, vol. 280, p. 115703, 2022.
- [45] M. Niazmand, A. Maghsoudipour, M. Alizadeh, Z. Khahpour and A. Kariminejad, "Effect of dip coating parameters on microstructure and thickness of 8YSZ electrolyte coated on NiO-YSZ by sol-gel process for SOFCs applications," *Ceramics International*, vol. 48, no. 11, pp. 16091-16098, 2022.
- [46] M. Esfahani, A. Eshaghi and S. Bakhshi, "Transparent hydrophobic, self-cleaning, anti-icing and anti-dust nanostructured silica based thin film on cover glass solar cell," *Journal of Non-Crystalline Solids*, vol. 583, p. 121479, 2022.
- [47] O. Beldjebli, R. Bensaha and P. Panneerselvam, "Effect of both Sn doping and annealing temperature on the properties of dip-coated nanostructured TiO₂ thin films," *Journal of Inorganic and Organometallic polymers and materials*, vol. 32, pp. 1624-1636, 2022.

- [48] J. Both, G. Szabo, G. Katona and L. Muresan, "Tannic acid reinforced sol-gel silica coatings for corrosion protection of zinc substrates," *Materials chemistry and physics*, vol. 282, p. 125912, 2022.
- [49] P. Karasinski, C. Tyszkiewicz, R. Piramidowicz and A. Kazmierczak, "Development of integrated photonics based on SiO₂:TiO₂ sol-gel derived waveguide layers:state of the art, perspectives, prospective applications," in *Proc. SPIE 11364, Integrated Photonics Platforms: Fundamental Research, Manufacturing and Applications, 1136414*, SPIE Photonics Europe, 2020.
- [50] P. Hermann and D. Wildmann, "Fabrication of planar dielectric waveguides with high optical damage threshold," *IEEE Journal of Quantum Electronics*, vol. 19, no. 12, pp. 1735-1738, 1983.
- [51] W. Lukosz and K. Tiefenthaler, "Embossing technique for fabricating integrated optical components in hard inorganic waveguiding materials," *Optics Letters*, vol. 8, pp. 537-539, 1983.
- [52] K. Tiefenthaler and W. Lukosz, "Sensitivity of grating couplers as integrated-optical chemical sensors," *J. Opt. Soc. Am. B*, vol. 6, pp. 209-220, 1989.
- [53] D. Clerc and W. Lukosz, "Direct immunosensing with an integrated-optical output grating coupler," *Sensors and Actuators B*, vol. 40, pp. 53-58, 1997.
- [54] Z. Jiwei, Y. Xi and Z. Liangying, "Characterization and optical propagation loss of sol-gel derived TiO₂/SiO₂ films," *J. Phys. D: Appl. Phys.*, vol. 33, pp. 3013-3017, 2000.
- [55] K. Tiefenthaler, V. Briguët, E. Buser, M. Horisberger and W. Lukosz, "Preparation of planar optical SiO₂-TiO₂ and LiNbO₃ waveguides with a dip coating method and embossing technique for fabricating grating couplers and channel waveguides," *Proc. SPIE*, vol. 401, pp. 165-173, 1983.
- [56] P. Chrysicopoulou, D. Davazoglou, C. Trapalis and G. Kordas, "Optical properties of SiO₂-TiO₂ sol-gel thin films," *Journal of Materials Science*, vol. 39, pp. 2835-2839, 2004.
- [57] X. Wang, G. Wu, B. Zhou and J. Shen, "Thermal annealing effect on optical properties of binary TiO₂-SiO₂ sol-gel coatings," *Materials*, vol. 6, pp. 76-84, 2013.
- [58] S. Kermadi, N. Agoudjil, S. Sali, L. Zougar, M. Boumaour, L. Broch and F. Placido, "Microstructure and optical dispersion characterization of nanocomposite sol-gel TiO₂ -SiO₂ thin films with different compositions," *Spectrochimica Acta Part A: Molecular and Biomolecular Spectroscopy*, vol. 145, pp. 145-154, 2015.
- [59] A. Lukowiak, R. Dylewicz, S. Patela, W. Strek and K. Maruszewski, "Optical properties of SiO₂-TiO₂ thin film waveguides obtained by the sol-gel method and their applications for sensing purposes," *Optical Materials*, vol. 27, pp. 1501-1505, 2005.
- [60] R. Almeida, P. Morais and H. Vasconcelos, "Optical loss mechanism in nanocomposite sol-gel planar waveguides," in *Proc. SPIE, Sol-Gel Optics IV*, pp. 296-303, 1997.
- [61] L. Weisenbacht and B. Zelinski, "The attenuation of sol-gel waveguides measured as a function of wavelength and sample age," in *Proc. SPIE 2288 Sol-Gel Optics III*, pp. 630-639, 1994.
- [62] P. Karasinski, C. Tyszkiewicz, A. Domanowska, A. Michalewicz and J. Mazur, "Low loss, long time stable sol-gel derived silica-titania waveguide films," *Materials Letters*, vol. 143, pp. 5-7, 2015.
- [63] Y. Enami , "Fabricating 90 nm resolution structures in sol-gel silica optical waveguides for biosensor applications," *Journal of Sensors*, vol. 2017, p. 4198485, 2017.
- [64] L. Blankenburg, K. Schultheis, H. Schache, S. Sensfuss and M. Schrodner, "Reel-to-reel wet coatings as an efficient up-scaling technique for the production of bulk-heterojunction polymer solar cells," *Solar Energy Materials & Solar Cells*, vol. 93, pp. 476-483, 2009.

- [65] A. Emslie, F. Bonner and L. Peck, "Flow of a viscous liquid on a rotating disk," *Journal of Applied Physics*, vol. 29, p. 858, 1958.
- [66] Y.-Y. Huang and K.-S. Chou, "Studies on the spin coating process of silica films," *Ceramics International*, vol. 29, no. 5, pp. 485-493, 2003.
- [67] P. Burmann, B. Zornoza, C. Tellez and J. Coronas, "Mixed matrix membranes comprising MOFs and porous silicate fillers prepared via span coating for gas separation," *Chemical Engineering Science*, vol. 107, pp. 66-75, 2014.
- [68] M. Hashizume and T. Kunitake, "Preparation of Self-Supporting Ultrathin Films of Titania by Spin Coating," *Langmuir*, vol. 19, no. 24, pp. 10172-10178, 2003.
- [69] Y. Xie, F. Zabihi and M. Eslamian, "Fabrication of highly reproducible polymer solar cells using ultrasonic substrate vibration posttreatment," *J. of Photonics for Energy*, vol. 6, no. 4, p. 045502, 2016.
- [70] D. Coyle, C. Macosko and L. Scriven, "Film-splitting flows in forward roll coating," *J. Fluid Mech.*, vol. 171, pp. 183-207, 1986.
- [71] J. Hintermaier and R. White, "The splitting of a water film between rotating rolls," *TAPPI J.*, vol. 48, pp. 617-625, 1965.
- [72] H. Benkreira, M. Edwards and W. Wilkinson, "A semi-empirical model of the forward roll coating flow of Newtonian fluids," *Chem. Eng. Sci.*, vol. 36, pp. 423-427, 1981.
- [73] H. Benkreira, M. Edwards and W. Wilkinson, "Roll coating of purely viscous liquids," *Chem. Eng. Sci.*, vol. 36, pp. 429-434, 1981.
- [74] H. Benkreira, M. Edwards and W. Wilkinson, "Roll coating operations," *J. Non-Newton. Fluid Mech.*, vol. 14, pp. 377-389, 1984.
- [75] H. Benkreira, R. Patel, M. Edwards and W. Wilkinson, "Classification and analyses of coating flows," *J. Non-Newton. Fluid Mech.*, vol. 54, pp. 437-447, 1994.
- [76] S. Sofou and E. Mitsoulis, "Roll-over-web coating of pseudoplastic and viscoplastic sheets using the lubrication approximation," *J. Plast. Film Sheet*, vol. 21, pp. 307-333, 2005.
- [77] M. Zahid, T. Haroon, M. Rana and A. Siddiqui, "Roll coating analysis of a third grade fluid," *J. Plast. Film Sheet.*, vol. 33, pp. 72-91, 2017.
- [78] M. Zahid, M. Rana and A. Siddiqui, "Roll coating analysis of a second-grade material," *J. Plast. Film Sheet*, vol. 34, pp. 232-255, 2018.
- [79] N. Ali, H. Atif, M. Javed and M. Sadiq, "A theoretical analysis of roll-over-web coating of couple stress fluid," *J. Plast. Film Sheet.*, vol. 34, pp. 43-59, 2018.
- [80] P. Gaskell, M. Savage, J. Summers and H. Thompson, "Modelling and analysis of meniscus roll coating," *J. Fluid Mech.*, vol. 298, pp. 113-137, 1995.
- [81] V. Marinca and N. Herisanu, "Determination of periodic solutions for the motion of a particle on a rotating parabola by means of the optimal homotopy asymptotic method," *J. Sound Vib.*, vol. 329, pp. 1450-1459, 2010.
- [82] M. Zhai, Y. Liu, J. Huang, W. Hou, S. Wu, B. Zhang and H. Li, "Fabrication of TiO₂-SrCO₃ composite coatings by suspension plasma spraying: microstructure and enhanced visible light photocatalytic performances," *J. Therm Spray Technol.*, vol. 29, pp. 1172-1182, 2020.
- [83] M. Gardon and J. Guilemany, "Milestones in functional titanium dioxide thermal spray coatings: a review," *J. Therm Spray Technol.*, vol. 23, pp. 577-595, 2014.

[84] F. Li, X. Lan, L. Wang, X. Kong, P. Xu, Y. Tai, G. Liu and J. Shi, "An efficient photocatalyst coating strategy for intimately coupled photocatalysis and biodegradation (ICPB) powder spraying method," *Chem Eng J.*, vol. 383, p. 123092, 2020.

[85] S. Santos, L. Paulista, T. Silva, M. Dias, J. Lopes, R. Boaventura and V. Vilar, "Intensifying heterogeneous TiO₂ photocatalysis for bromate reduction using the NETmix photoreactor," *Sci. Total Environ.*, vol. 664, pp. 805-816, 2019.

[86] F. Montecchio, D. Chinungi, R. Lanza and K. Engvall, "Surface treatments of metal supports for photocatalysis applications," *Appl. Surf. Sci.*, vol. 401, pp. 283-296, 2017.

[87] M. Bousmaha, M. Bezzerrouk, B. Kharroubi, A. Akriche, R. Naceur, I. Hattabi and K. Sandjak-Eddine, "Enhanced photocatalysis by depositing ZnO thin film in the inner wall of glass tube," *Optik*, vol. 183, pp. 727-731, 2019.

[88] G. Susanna, L. Salamandra, T. Brown, A. Carlo, F. Brunetti and A. Reale, "Airbrush spray-coating of polymer bulk-heterojunction solar cells," *Solar Energy Materials and Solar Cells*, vol. 95, no. 7, pp. 1775-1778, 2011.

[89] S.-Y. Park, Y.-J. Kang, S. Lee, D.-G. Kim, J.-K. Kim, J. Kim and J.-W. Kang, "Spray-coated organic solar cells with large-area of 12.25 cm²," *Solar Energy Materials and Solar Cells*, vol. 95, no. 3, pp. 852-855, 2011.

[90] S. Liu, X. Zhang, L. Zhang and W. Xie, "Ultrasonic spray coating polymer and small molecular organic film for organic light-emitting devices," *Scientific Reports*, vol. 6, p. 37042, 2016.

[91] M. Habibi, M.-R. Ahmadian-Yazdi and M. Eslamian, "Optimization of spray coating for the fabrication of sequentially deposited planar perovskite solar cells," *J. Photon. Energy*, vol. 7, no. 2, p. 022003, 2017.

[92] M. Xiao, F. Huang, W. Huang, Y. Dkhissi, Y. Zhu, J. Etheridge, A. Gray-Weale, U. Bach, Y.-B. Cheng and L. Spiccia, "A fast deposition-crystallization procedure for highly efficient lead iodide perovskite thin-film solar cells," *Angew Chem Int Ed Engl.*, vol. 53, no. 37, pp. 9898-9903, 2014.

[93] N. Jeon, J. Noh, Y. Kim, W. Yang, S. Ryu and S. Seok, "Solvent engineering for high-performance inorganic-organic hybrid perovskite solar cells," *Nat. Mater.*, vol. 13, no. 9, pp. 897-903, 2014.

[94] Jeong, J; et al. , "Pseudo-halide anion engineering for alpha-FAPbI₃ perovskite solar cells," *Nature*, vol. 592, pp. 381-385, 2021.

[95] J. Qi, Z. Yang, Z. Xingwang, Y. Xiaolei, C. Yong, C. Zema, Y. Qiufeng, L. Xingxing, Y. Zhigang and Y. Jingbi, "Surface passivation of perovskite film for efficient solar cells," *Nature Photonics*, vol. 13, no. 7, pp. 460-466, 2019.

[96] X. Gu, L. Shaw, K. Gu, M. Toney and Z. Bao, "The meniscus-guided deposition of semiconducting polymers," *Nature Communications*, vol. 9, p. 534, 2018.

[97] D. Li, D. Zhang, K.-S. Lim, Y. Hu, Y. Rong, A. Mei, N.-G. Park and H. Han, "A review on scaling up perovskite solar cells," *Advanced Functional Materials*, vol. 31, no. 12, p. 2008621, 2021.

[98] Y. Deng, E. Peng, Y. Shao, Z. Xiao, Z. Dong and J. Huang, "Scalable fabrication of efficient organolead trihalide perovskite solar cells with doctor-bladed active layers," *Energy & Environment Science*, vol. 8, pp. 1544-1550, 2015.

[99] Razza, S; et al., "Perovskite solar cells and large area modules (100 cm²) based on an air flow-assisted PbI₂ blade coating deposition process," *Journal of Power Sources*, vol. 277, pp. 286-291, 2015.

[100] D. Vak, K. Hwang, A. Faulks, Y.-S. Jung, N. Clark, D.-Y. Kim, G. Wilson and S. Watkins, "Solar cells: 3D printer based slot-die coater as a lab-to-fab translation tool for solution-processed solar cells," *Advanced Energy Materials*, vol. 5, no. 4, pp. 1-8, 2015.

[101] Z. Wei, H. Chen, K. Yan and S. Yang, "Inkjet printing and instant chemical transformation of a CH₃NH₃PbI₃/nanocarbon electrode and interface for planar perovskite solar cells," *Angew Chem Int Ed Engl.*, vol. 53, no. 48, pp. 13239-13243, 2014.

[102] J. Heo, M. Lee, M. Jang and S. Im, "Highly efficient CH₃NH₃PbI_{3-x}Cl_x mixed halide perovskite solar cells prepared by re-dissolution and crystal grain growth via spray coating," *Journal of Materials Chemistry A*, vol. 4, pp. 17636-17642, 2016.

[103] A. Schneider, N. Traut and M. Hamburger, "Analysis and optimization of relevant parameters of blade coating and gravure printing processes for the fabrication of highly efficient organic solar cells," *Solar Energy Materials and Solar Cells*, vol. 126, pp. 149-154, 2014.

[104] Tsai, P-T; Tsai, C-Y; et al., "High-efficiency polymer solar cells by blade coating in chlorine-free solvents," *Organic Electronics*, vol. 15, no. 4, pp. 893-903, 2014.

[105] Y.-H. Chang, S.-R. Tseng, C.-Y. Chen, H.-F. Meng, E.-C. Chen, S.-F. Horng and C.-S. Hsu, "Polymer solar cell by blade coating," *Organic Electronics*, vol. 10, no. 5, pp. 741-746, 2009.

[106] S. Siegrist, S.-C. Yang, E. Gilshtein, X. Sun, A. Tiwari and F. Fu, "Triple-cation perovskite solar cells fabricated by a hybrid PVD/blade coating process using green solvents," *J. Mater. Chem. A*, vol. 9, p. 26680, 2021.

[107] A. Jilani, M. S. Abdel-Wahab and A. H. Hammad, "Advance deposition techniques for thin film and coating," in *Modern technologies for creating the thin film systems and coatings*, IntechOpen, 2017, pp. 137-149.

[108] Butt, M.A; et al., "Optical Thin Films Fabrication Techniques—Towards a Low-Cost Solution for the Integrated Photonic Platform: A Review of the Current Status," *Materials*, vol. 15, no. 13, p. 4591, 2022.

[109] S. Boolchandani, S. Srivastava and Y. K. Vijay, "Preparation on InSe thin films by thermal evaporation method and their characterization: Structural, optical, and thermoelectrical properties," *Journal of Nanotechnology*, vol. 2018, p. 9380573, 2018.

[110] N. Ali, J. A. Teixeira, A. Addali, M. Saeed, F. Al-Zubi, A. Sedaghat and H. Bahzad, "Deposition of stainless steel thin films: An electron beam physical vapour deposition approach," *Materials*, vol. 12, p. 571, 2019.

[111] S. N. Ogugua, O. M. Ntwaeborwa and H. C. Swart, "Latest development on pulsed laser deposited thin films for advanced luminescence applications," *Coatings*, vol. 10, p. 1078, 2020.

[112] M. Opel, S. Geprags, M. Althammer, T. Brenninger and R. Gross, "Laser molecular beam epitaxy of ZnO thin films and heterostructures," *Journal of Physics D: Applied Physics*, vol. 47, p. 034002, 2014.

[113] P. M. Martin, "Handbook of deposition technologies for films and coatings (Third edition)," in *Science, Applications and Technology*, Elsevier Inc., 2010, pp. 297-313.

[114] H. S. Randhawa, R. F. Bunshah, D. G. Brock, B. M. Basol and O. M. Stafsudd, "Preparation of Cu_xS thin films by activated reactive evaporation technique," *Solar Energy Materials*, vol. 6, no. 4, pp. 445-453, 1982.

[115] N. Woehrl, O. Ochedowski, S. Gottlieb, K. Shibusaki and S. Schulz, "Plasma-enhanced chemical vapor deposition of graphene on copper substrates," *AIP Advances*, vol. 4, p. 047128, 2014.

[116] A. Cohen, A. Patsha, P. K. Mohapatra, M. Kazes, K. Ranganathan, L. Houben, D. Oron and A. Ismach, "Growth-etch metal-organic chemical vapor deposition approach of WS₂ atomic layers," *ACS Nano*, vol. 15, no. 1, pp. 526-538, 2021.

[117] H. Okada, M. Baba, M. Furukawa, K. Yamane, H. Sekiguchi and A. Wakahara, "Formation of SiO₂ film by chemical vapor deposition enhanced by atomic species extracted from a surface-wave generated plasma," *AIP Conference Proceedings*, vol. 1807, p. 020006, 2017.

- [118] Y. Matsuura and J. A. Harrington, "Hollow glass waveguides with three-layer dielectric coating fabricated by chemical vapor deposition," *Journal of the Optical Society of America A*, vol. 14, no. 6, pp. 1255-1259, 1997.
- [119] Y. Matsuura and J. A. Harrington, "Infrared hollow glass waveguides fabricated by chemical vapor deposition," *Optics Letters*, vol. 20, no. 20, pp. 2078-2080, 1995.
- [120] J. K. Saha, R. N. Bukke, N. N. Mude and J. Jang, "Significant improvement of spray pyrolyzed ZnO thin film by precursor optimization for high mobility thin film transistors," *Scientific Reports*, vol. 10, p. 8999, 2020.
- [121] G. E. Patil, D. D. Kajale, V. B. Gaikwad and G. H. Jain, "Spray pyrolysis deposition of nanostructured tin oxide thin films," *International Scholarly Research Notices*, vol. 2012, p. 275872, 2012.
- [122] J. Cho, S. Hwang, D.-H. Ko and S. Chung, "Transparent ZnO thin-film deposition by spray pyrolysis for high-performance metal-oxide field-effect transistors," *Materials*, vol. 12, no. 20, p. 3423, 2019.
- [123] L. Filipovic, S. Selberherr, G. C. Mutinati, E. Brunet, S. Steinhauer, A. Kock, J. Teva, J. Kraft, J. Siegert and F. Schrank, "Methods of simulating thin film deposition using spray pyrolysis techniques," *Microelectronic Engineering*, vol. 117, pp. 57-66, 2014.
- [124] M. F. Ramadhan, M. H. Pasaribu, B. Yuliarto and Nugraha, "Fabrication of ZnO nanorod using spray-pyrolysis and chemical bath deposition method," *AIP Conference Proceedings*, vol. 1586, p. 74, 2014.
- [125] J. Whitaker, D. Kim, B. Larson, F. Zhang, J. Berry, M. Hest and K. Zhu, "Scalable slot-die coating of high performance perovskite solar cells," *Sustainable Energy & Fuels*, vol. 2, pp. 2442-2449, 2018.